Using the Mohr-Coulomb Criterion to Estimate Shear Strength of RC Columns

Santiago Pujol, Nobuaki Hanai, Toshikatsu Ichinose and Mete A. Sozen

Biography: Santiago Pujol, FACI, is an Associate Professor at the Lyles School of Civil Engineering at Purdue University, IN. He received his BS from Universidad Nacional de Colombia at Medellín in 1996 and his MS and PhD from Purdue University in 1997 and 2002. He is a member of ACI committees 318r, 314, 445, and 133. He received the W. L. Huber Research award of ASCE in 2012. His research interests include seismic response of reinforced concrete structures. **Nobuaki Hanai** is a Professor at Department of Architecture at Kyushu Sangyo University, Fukuoka, JAPAN. He received his BE, ME, and DE from Nagoya Institute of Technology, Nagoya, JAPAN, in 1998, 2000, and 2007, respectively. He is a member of the committee of AIJ RC building code. He received the encouragement award of JCI in 2004. His research interests include seismic design of reinforced concrete structures. ACI member **Toshikatsu Ichinose** is a Professor at Department of Architecture at Nagoya Institute of Technology. He received his BE from Nagoya Institute of Technology in 1977 and his ME and DE from the University of Tokyo, Tokyo, JAPAN, in 1979 and 1982, respectively. He chairs the committee of AIJ RC building code. He received the research awards of AIJ and JCI in 1998 and 2015, respectively. His research interests include seismic design of reinforced concrete structures. **Mete A. Sozen**, Kettelhut Distinguished Professor of Structural Engineering at Purdue University, is an honorary member of the American Concrete Institute, American Society of Civil Engineers, and the Architectural Institute of Japan. He has been elected to membership in the U.S. National Academy of Engineers and the Royal Swedish Academy of Engineering

Sciences. He has been granted honorary doctorates by Bogazici University, TURKEY, Pannonius University, HUNGARY, The Georgian Technical University, Tbilisi, GEORGIA. He has received the Diogenes Award of the Colombian Association of Earthquake Engineering.

Abstract

An expression to estimate the unit shear strength of reinforced concrete columns is developed and calibrated using results from 62 tests on reinforced concrete members with rectangular cross sections. The effects of longitudinal reinforcement, transverse reinforcement, and axial load on shear strength are estimated with a simple formulation based on the Mohr-Coulomb failure criterion. It is concluded that shear strength increases at a decreasing rate with increases in transverse reinforcement and axial force.

Keywords: Mohr's circle, Coulomb criterion, shear failure, reinforced concrete, and column.

Introduction

A key to the survival of a reinforced concrete frame in an earthquake is prevention of shear failure in columns. The literature on the subject is rich. Nevertheless, the efforts to provide an answer to the riddle of shear strength have not converged to a generally accepted solution. In this study, the question of shear strength is re-examined by going back to a method that endured the test of time. Mohr's circle and Coulomb's failure criterion, which have been used for discontinuous materials such as soils, provide the basis for a simple formulation calibrated using results from sixty-two tests on reinforced concrete members that failed in shear before flexural yielding occurred. The test specimens had concrete strengths ranging from 2 to 14 ksi (14 to 99 MPa) and transverse reinforcement strengths ranging from 36 to 205 ksi (250 to 1413 MPa). The expression resulting from this study indicates that shear strength increases at a decreasing rate with increases in transverse reinforcement.

Works that have motivated the development of the analytical model include those of Mohr[1], Richart[2], Nielsen[3], and Mac Gregor[4].

Research Significance

A new formulation is developed to estimate the shear strength of reinforced concrete columns with closed ties. It was developed making use of a simple tool to tackle a complex problem. Mohr's circle enables quantification of the effects of forces in three dimensions. Used in combination with Coulomb's failure criterion, it provides a simple vehicle to account for the effects of confinement and axial load on shear strength. Within the ranges of the variables included in the database considered, the proposed procedure can serve as a simple and reliable design method.

Failure Criterion

The failure criterion is defined in Fig. **1**. Failure occurs if the stress circle reaches the boundary described by limits 1 and 2. Limit 1 in Fig. **1** refers to a classic in reinforced concrete literature: F. E. Richart's "Failure of Plain and Spirally Reinforced Concrete in Compression[2]". Richart concluded that the axial strength (σ_1) of normal-weight concrete cylinders (Fig. 2a) subjected to monotonically increasing load and transverse (confining) stress (σ_2) is approximately:

$$\sigma_1 = f'_c + 4\sigma_2 \qquad (1)$$

This equation describes a family of circles of diameter $f'_c + 3\sigma_2$ and center $(f'_c + 5\sigma_2)/2$ in the normal stress-shear stress plane (Fig. **2**b). The tangent to these circles (the broken line in Fig. **2b**) is:

$$\tau = k_1 f'_c + k_2\sigma \qquad (2)$$

where k_1 = 1/4 and k_2 = 3/4. The first factor k_1 represents cohesion and the second factor k_2 represents the coefficient of friction. σ and τ in Eq. 2 represent the stresses on the potential failure plane shown in Fig. 2a. On the other hand, tests for sand indicate $k_1 = 0$ and $k_2 \approx 3/4$ (Fig. **3a**). It is therefore assumed that k_2 = 3/4 is valid even in cracked concrete (Fig. **3b**) but k_1 is assumed to be 1/6, which is 2/3 (=0.67) of the value inferred from Richart's work for concentrically loaded specimens. The ratio of 0.67 can be considered to be an "effectiveness factor" similar, in concept and magnitude, to the factor $\nu = 0.8 - \frac{f'_c}{200}$ (MPa) proposed by Nielsen[3], which provides $\nu = 0.65$ for f'_c = 30 MPa. In Eq. 2, f'_c is the strength of unconfined concrete. Strictly, the term f'_c should refer to the strength of the concrete in the column, not to cylinder

strength. To keep the formulation simple, no distinction is made between the strength of the concrete in the column and cylinder strength. It could also be assumed that the 2/3 "effectiveness factor" accounts for the difference between column and cylinder concrete strength.

Limit 2 in Fig. **1** refers to tensile stresses in the concrete. It is assumed that tensile stresses in concrete do not exceed $f_t = \sqrt{f'_c}$ for f'_c and f_t in psi ($\frac{1}{12}\sqrt{f'_c}$ for f'_c and f_t in MPa). Limit 2 is a limit on average, or "smeared", tensile stresses (Vecchio and Collins[5]).

To illustrate the plausibility of the chosen limit on tensile stress, Figure **4a** shows an idealized column segment with shear cracks and light confinement. Figure **4b** shows a horizontal section of this segment. The small arrows in Figure **4b** represent bond stresses between the reinforcement and concrete. Figure **4** depicts the idealized stresses in the concrete core of a column. Consider the highlighted segment in Figure **4b**. Ties crossing the cracks that bound this segment are in tension. Part of that tension is transferred to the concrete through bond stresses (small arrows in Fig. **4b**). The resulting tensile stresses in the concrete are likely to increase towards the center of the segment (line CD) as the force transferred by the ties builds up (Figure **4c**). The maximum tensile stress in the concrete is unlikely to exceed its strength in direct tension[5] $f_{cr} = 4\sqrt{f'_c}$. If the ties are located along the periphery, then it follows that concrete tensile stresses are likely to be smaller away from the periphery where there is no force transferred from ties (Figure **4d**). The resulting state of stresses is idealized in Figures **4e** to **4g**. Figure **4g** shows an isometric view of the assumed tensile stress distribution. Figure **4g** illustrates that it is plausible that the average tensile stress in the concrete is only a fraction of the tensile strength. Noting that the average height of the pyramid shown in Fig. **4h** is $f_{cr}/3$, this fraction is approximated here as $f_t = \frac{f_{cr}}{4} = \sqrt{f'_c}$ (psi).

Definition of Unit Stresses

Having defined a failure criterion, we need to define the required unit stresses. The distributions of unit shear and normal stresses in a cracked reinforced concrete element under shear reversals defy exact determination. No attempt is made to estimate stresses exactly. Instead, the mean axial stress (Fig. **5c**) is assumed to be:

$$\sigma_a = \frac{P+T}{A_c} \tag{3}$$

The force P is axial load, the area A_c is the cross-sectional area of the concrete core (measured from center to center of outermost legs of hoops) and the force T is assumed to be given by the following expression as discussed later in this section:

$$T = \frac{1}{4} A_{st} f_y \left(1 - \frac{P}{0.3 f'_c A_g} \right) \tag{4}$$

A_{st} is the total cross-sectional area of longitudinal reinforcement, f_y is the yield stress of longitudinal reinforcement, A_g is gross cross-sectional area, and f'_c is concrete strength.

T is the resultant of forces in the longitudinal steel reinforcement. Eq. 4 provides an estimate of T without unwarranted computational effort. Figures **6a** and **6b** show results from Eq. 4 compared with values estimated for a square cross section with 2 and 4 layers of steel reinforcement. These values were obtained from sectional analyses made 1) to satisfy equilibrium at each column end, and 2) using the following assumptions:

Geometry

Longitudinal (or normal) strain is proportional to distance to neutral axis

Maximum longitudinal (normal) compressive strain ranges from 0.001 to 0.003

Concrete

Compressive strength is 4ksi (reached at a strain equal to 0.002)

Stress strain curve follows the relationship proposed by Hognestad

Steel

Steel is elasto-plastic

Yield stress is 60ksi

Modulus of Elasticity is 29,000ksi

Proportions

Total steel area is 1.5% (2 layers) or 2% (4 layers) of total gross cross-sectional area

Figures **6a** and **6b** show that the results from Eq. 4 are plausible especially for sections with smaller concrete strains (which is likely to be the case for columns that fail in shear before yielding of longitudinal reinforcing bars).

The focus of this article is on columns with rectangular cross sections and hoops. Therefore, mean transverse stress (Fig. **5b**) is defined as:

$$\sigma_t = p_{we}\, f_{yt} \tag{5}$$

The ratio $p_{we} = A_{sh}/(b_c\, s)$ refers to transverse reinforcement (cross-sectional area of transverse reinforcement A_{sh} divided by the product of core width b_c times stirrup spacing s) and f_{yt} is the yield stress of the transverse reinforcement. The confinement from beam column joints is ignored.

Mean unit shear stress (Fig. **5a**) is defined as:

$$\tau = \frac{V}{A_c} \tag{6}$$

V is the shear force at failure and A_c is the cross-sectional area of the core. We solve for the unit shear strength by constructing a Mohr circle in which the normal stresses σ_a and σ_t are fixed.

1 And we vary the radius of the circle to find the maximum shear stress that can be "tolerated"
2 before the circle reaches the limits defined in Fig. **1**. There are two possibilities: (a) limit 1
3 controls (Fig. **7a**), and (b) limit 2 controls (Fig. **7b**). We assume that, because our focus is on
4 columns that do not reach yielding of the longitudinal reinforcement, the failure envelope is not
5 sensitive to number of load reversals and, therefore, we do not attempt to make the coefficients
6 in Eq. 2 functions of number of cycles or displacement.

7 The solution for case (a) is: $\tau_1 = \frac{1}{5}\sqrt{\left(\frac{2}{3} f_c' + 4\sigma_a - \sigma_t\right)\left(\frac{2}{3} f_c' - \sigma_a + 4\sigma_t\right)}$ (7)

8 The solution for case (b) is: $\tau_2 = \sqrt{(\sigma_a + f_t)(\sigma_t + f_t)}$ (8)

9

10 ## Results

11 The expression described was calibrated using data from 62 tests[6-20]. All the test
12 specimens were loaded uniaxially, were reported to have failed in shear before flexural yielding,
13 and had strengths smaller than computed flexural strengths. Table 1 summarizes the properties
14 of the specimens considered. The ranges of the variables included in these tests are:

15 Concrete strength (from 4x8 in. or 6x12 in. cylinders):2 to 14 ksi (14 to 99 MPa)
16 Yield stress of longitudinal reinforcement: 48 to 157 ksi (331 to 1080 MPa)
17 Yield stress of transverse reinforcement: 36 to 205 ksi (250 to 1413 MPa)
18 Longitudinal reinforcement ratio: 1.6 to 5.4 %
19 Transverse reinforcement ratio ($p_{we} = A_{st} / b_c s$): 0.0 to 1.7 %
20 Axial load ratio: 0 to 0.61

Ratio of shear span[1] to effective depth:	1.1 to 4.05
Shear stress at failure:	250 to 2800 psi (1.7 to 19 MPa)
Number of cycles applied before failure:	0 to 8
Number of elements tested in single curvature:	3
Number of elements tested in double curvature:	59

Before describing the results of the proposed expression for the entire database, the effects of the amounts and yield strength of transverse reinforcement on shear strength are considered. Fukuhara[20] subjected beams to monotonically increasing shear forces and double curvature. Details of the specimens are listed in Table 1. Measured shear force at failure, normalized with respect to the area of the concrete core (measured from center to center of opposite legs of peripheral hoops) is plotted against σ_t in Figure **8**. The trend revealed by Fukuhara's tests is clear. It indicates that increase in transverse reinforcement increases shear strength at a decreasing rate. Japanese design recommendations (Arakawa[21]) account for this effect by assuming that the fraction of the shear strength attributable to transverse reinforcement is proportional to

$$\sqrt{\frac{A_{sh}}{b \cdot s} f_{yt}}$$

ACI-318[22] recommendations for design assume the contribution from transverse reinforcement to shear strength to be proportional to

$$\frac{A_{sh}}{b \cdot s} f_{yt}$$

---

[1] Shear span is the distance between the inflection point and the point of the maximum bending moment in the column.

ACI-318[22] recommendations reflect the decrease in the effectiveness of the transverse reinforcement mentioned by introducing a limit for the maximum shear force that can be attributed to the transverse reinforcement V_s ($2/3\sqrt{f'_c}\times b\ d$ for MPa, $8\sqrt{f'_c}\times b\ d$ for psi). The thick broken line in Fig. **8** represents results from expressions 22-5-1-1, 22-5-6-1, 22-5-10-5-3 and the limit in section 22.5.1.2 of the ACI-318-14 design recommendations[22]:

$$V_n = V_c + V_s \qquad (22\text{-}5\text{-}1\text{-}1)$$

$$V_c = 2\left(1+\frac{P}{2000\text{psi}\times A_g}\right)\sqrt{f'_c}\times b\cdot d \qquad (22\text{-}5\text{-}6\text{-}1)$$

$$V_s = A_{sh} f_{yt}\frac{d}{s} \qquad (22\text{-}5\text{-}10\text{-}5\text{-}3)$$

$$V_s \le 8\sqrt{f'_c\cdot\text{psi}} \qquad (22.5.1.2)$$

(These expressions have been rewritten using the notation adopted in this paper)

The horizontal segment of the thick broken line in Fig. **8** is associated with the limit imposed on V_s. The ACI-318[22] procedure is successful because it is simple and conservative. The results obtained with the approach proposed are represented by the continuous line in Fig. **8**. Limit 2 controls for $0 \le p_{we} f_{yt} \le 8$ MPa and Limit 1 controls for $p_{we} f_{yt} \ge 8$ MPa. The results follow the experimental data closely. Nevertheless, what is of interest is the trend: the nonlinearity in the relationship between shear strength and transverse reinforcement strength. This nonlinearity is inherent in the failure criterion adopted. Consider the Mohr circles illustrated in Figure **9**. Each circle represents a column subjected to axial stress σ_a and transverse stress σ_t. The axial stress is the same for all circles. The transverse stress changes from circle to circle in increments of constant magnitude $\Delta\sigma_t$. The radius of each circle has been adjusted so that all the circles are tangent to the failure surface. The circles drawn in broken lines are tangent to Limit 1. The solid

circles are tangent to Limit 2. In each circle, the vertical coordinate τ of the point in the upper-right quadrant with a normal stress σ_t represents unit shear strength. Figure **9** shows that successive increments in σ_t result in increments in shear strength of decreasing magnitude. The points with coordinates τ and σ_t in this plot represent, schematically, the solution shown in Fig. **8**.

For reference, Figure **8** includes results obtained using the upper-bound solution (the plasticity theorem) by Nielsen[3] for a/h = 1.0 and f_c' = 28 MPa. Results for a/h = 1.5 and f_c' = 32 MPa are similar and are not shown for clarity. This solution produced increases in estimated shear strength with increasing transverse stress up to 9.3 MPa (which is a half the effective compressive strength of cracked concrete $\nu.f'_c/2$) suggesting shear-compression controls if large amounts of transverse reinforcement are used. Figure **8** also includes results obtained using the software package Response-2000[23], which is based on the modified compression field theory by Vecchio et al[5]. The upper limit of the curve for a/h = 1.0 is equal to $f_{2max}/2$, implying again that shear-compression failure may occur before yielding of transverse reinforcement. The results obtained for a/h = 1.0 are larger than the measured stresses. This was to be expected because Response-2000 has been reported[23] to produce poor results for $a=M/V<d$. The curve for a/h = 1.5 provides a better match with test results. The upper limit of this curve is equal to the flexural strength of the specimen.

Next, the effect of axial load is studied. Table 22.5.6.1 of ACI-318[22] includes terms related to axial load that are more elaborate –and presumably more reliable– than Eq. 22-5-6-1. Shear strength was calculated using these equations (ACI-318[22] Table 22.5.6.1a) and the procedure proposed here. Table 22.5.6.1(a) and limits associated with it are rewritten here as follows:

$$V_c = 1.9\sqrt{f'_c} + 2500\text{psi} \times \rho_w \times \frac{d}{a - \frac{P}{V_n}\left(\frac{4h-d}{8}\right)} \qquad \text{Table 22.5.6.1a}$$

$$a - \frac{P}{V_n}\left(\frac{4h-d}{8}\right) > 0 \qquad \text{Table 22.5.6.1(a)}$$

$$V_c \le 3.5\sqrt{f'_c \cdot \text{psi}}\sqrt{1 + \frac{P}{500\text{psi} \times A_g}} \times b \cdot d \qquad \text{Table 22.5.6.1(b)}$$

Figure **10** shows the mean ratio of measured to computed strength plotted against axial load ratio for 62 experiments. The thick line in Fig. **10a** shows the mean ratio of measured to computed strength plotted versus axial load ratio. Although the ACI-318[22] expressions are not meant to produce "average" values to be compared directly to tests data, it is interesting to note that there is a slight tendency for Table 22.5.6.1(a)to produce larger values of computed strength for $\frac{P}{f'_c \times A_g} > 0.2$. Such a tendency is not observed in Fig. **10b** for the proposed expression.

Figure **10b** indicates that the averages of the ratios of measured strength to strength calculated using the proposed procedure are close to 1 in the ranges of axial load and aspect ratio considered. This result should have been expected because all the assumptions described in this article were conceived to lead to mean test results. For design, shear strength should be computed as:

$$\phi V_n = \phi\left(A_c \times \tau_n\right) \qquad (16)$$

Use of ϕ=2/3 provides a reasonable lower bound to shear strength.

Figure **11** shows projected shear strength for columns with:

a/d = 2

f'_c = 35MPa (5000psi)

$A_{st}/(b \cdot d)$ = 2%

f_y = 520MPa (75ksi)

f_{yt} = 410MPa (60ksi)

A_g/A_c = 1.5

h/d = 1.1

The ratio of transverse reinforcement p_{we} is varied between 0% and 1.5%. Three values of axial load ratio $P/(f'_c A_g)$ are considered: 0.1, 0.2, 0.3. Projections are made with the proposed method and Table 22.5.6.1(a). The results from the proposed method are multiplied by 2/3 in an attempt to make the comparison relevant for design and evaluation purposes. Figure **11** shows that the proposed procedure provides results with a smoother transition from small to large amounts (and/or strength) of transverse reinforcement, a transition that resembles that observed by Fukuhara[20] (Fig. **8**).

Limitations of the proposed procedure

Figure **12** shows the relationship between axial load ratio and estimated shear strength for various transverse reinforcement ratios and the parameters used for Fig. **11**. The curve for p_{we} = 0% drops drastically from point A to point B. Point B suggests that failure under concentric axial load (zero shear) would take place at a stress close to $f'_c/2$ (instead of f'_c). This projected decrease in axial strength is caused by:

1) the assumed "effectiveness factor" of 2/3 used to reduce k_1 in Eq. 2, and

2) ignoring the cover concrete (A_g/A_c = 1.5).

It is likely that, between points A, B and C in Fig. **12**, the effectiveness factor associated with Eq. 2 is larger than 2/3 because larger axial load may reduce the effects of shear stresses. It may be also be reasonable to expect the contribution of concrete cover to be more relevant than it

was assumed. Accounting for these two factors may result in a smoother decrease in strength from A to C. Similar smoother transitions (from shear to axial failures) are expected for the other cases shown in Fig. **12**. Nevertheless, it is unlikely that columns in practice will be designed to reach axial concrete stresses exceeding $f'_c/2$ (i.e. in the range between A and C).

Figure **13** shows ratios of measured to computed strength plotted against aspect ratio (a/d), where a is the shear span. The proposed expression does not include aspect ratio as a parameter. For the available data, the proposed procedure yields larger estimates of shear strength for columns with aspect ratios larger than 2.5 (mean measured-to-computed strength ratio = 0.75) than for columns with smaller aspect ratios (mean measured-to-computed strength ratio > 0.95) –Fig. **13b**–.

Conclusions

Mohr's circle has been used to interpret data from tests of reinforced concrete columns reported to fail in shear. In the proposed procedure, shear strength is to be computed from:

$$\phi V_n = \phi\left(A_c \times \tau_n\right) \qquad (16)$$

Use of $\phi = 1$ provides an estimate of mean shear strength and $\phi = 2/3$ provides a reasonable lower bound to shear strength. A_c is the cross-sectional area of the core (measured center-to-center of opposite legs of peripheral hoops). Unit shear stress τ_n is the smaller of τ_1 and τ_2, where τ_1 is determined by Eq. 7:

$$\tau_1 = \frac{1}{5}\sqrt{\left(\tfrac{2}{3} f'_c + 4\sigma_a - \sigma_t\right)\left(\tfrac{2}{3} f'_c - \sigma_a + 4\sigma_t\right)} \qquad (7)$$

and τ_2 is determined by Eq. 8:

$$\tau_2 = \sqrt{\left(\sigma_a + f_t\right)\left(\sigma_t + f_t\right)} \qquad (8)$$

The proposed expressions indicate that (1) shear strength increases at a decreasing rate with increases in transverse reinforcement, and (2) shear strength increases with increases in axial force for axial concrete stresses not exceeding approximately $0.4f'_c$. The proposed procedure may be too conservative for columns with axial force ratios larger than 0.4 and small amounts of transverse reinforcement. The proposed procedure may not always be conservative for columns with $a/d > 2.5$.

Notation

a :	Shear span
A_c :	Cross-sectional area of concrete core
A_g :	Cross-sectional area of gross section
A_s :	Area of longitudinal tension reinforcement
A_{sh} :	Area of transverse reinforcement
A_{st} :	Total area of longitudinal reinforcement
b :	Width of gross section
b_c :	Width of concrete core
d :	Effective depth
f'_c :	Concrete compressive strength
f_t :	Tensile stress limit ($f_t = \sqrt{f'_c}$ for psi, $f_t = \frac{1}{12}\sqrt{f'_c}$ for MPa)
f_y :	Yield stress of longitudinal reinforcement
f_{yt} :	Yield stress of transverse reinforcement
h :	Depth of gross section
h_c :	Depth of concrete core
k_1 :	"Cohesion" coefficient (assumed to be 1/6)
k_2 :	"Friction" coefficient (assumed to be 3/4)
P :	Axial force
$p_{we} = \frac{A_{sh}}{b_c s}$	Ratio of transverse reinforcement
s :	Spacing of transverse reinforcement
$T = 1/4 \cdot A_{st} \cdot f_y \, [1-P/(0.3 \cdot A_g \cdot f'_c)]$	Estimate of the force in the reinforcement in tension

V :	Shear force
V_c :	Shear strength attributed to concrete
V_n :	Nominal shear strength
V_s :	Shear strength attributed to transverse steel
ρ :	Ratio of longitudinal reinforcement (Total cross-sectional area of reinforcement divided by A_g)
ρ_w :	Ratio of longitudinal tension reinforcement $A_s/(b \times d)$
σ_1, σ_2 :	Principal unit stresses
$\sigma_a = [P+T]/A_c$	Average unit axial stress
$\sigma_t = p_{we} f_{yt}$	Average unit transverse stress
$\tau = V/A_c$:	Average unit shear stress
τ_n	Computed shear strength
τ_u	Measured shear strength

REFERENCES

[1] Mohr, O., "Welche Umstande bedingen die Elastizitatsgrenze und den Bruch eines Materials," Zeitschrift des Vereins Deutscher Ingenieure, 1900, p. 1524.

[2] Richart, F.E., Brandtzaeg, A., and Brown, R.L., "The Failure of Plain and Spirally Reinforced Concrete in Compression," Univ. of Illinois Eng. Exp. Station, Bulletin, No. 190, V. 26, No. 31, April, 1929, pp. 1-74.

[3] Nielsen, M. P.: *Limit Analysis and Concrete Plasticity*, CRC Press LLC, Boca Raton, Florida, USA, 1998, 908 p.

[4] Mac Gregor, J., Sozen, M. A., Siess, C. P.: "Strength of Prestressed Concrete Beams with Web Reinforcement," *ACI Journal Proceedings*, Vol. 62, No. 12, 1965, pp. 1503-1519.

[5] Vecchio, F.J.; Collins, M.P. (1986). "The Modified Compression-Field Theory for Reinforced Concrete Elements Subjected to Shear". *ACI Journal*. Vol. 83, No. 2, pp. 219–231.

[6] Hanai, N., Umemura, H., Ichinose, T.: "The Factors Which Influence Strength Deterioration of RC Columns Failing in Shear after Flexural Yielding," *J. Struct. Constr*. Eng., AIJ, No. 593, 2005, pp. 129-136 (in Japanese).

[7] Nishi, K., Ito, Y., Hanai, N., Ichinose, T.: "Deformation Capacity of RC Column Retrofitted with Aramid Fiber at Large Intervals," *Proceedings of the Japan Concrete Institute*, Vol. 28, No. 2, 2006, pp. 1429-1434 (in Japanese).

[8] Ishigami, S., Owa S., Nakamura, T., Yoshimura, M.: "Axial Load Carrying Capacity of Shear-Failing RC Columns Part 1-3," *Summaries of Technical Papers of Annual Meeting Architectural Institute of Japan*, C-2, 2002, pp. 391-396 (in Japanese).

[9] Takami, Yoshioka, K.: "Shear Strength of RC Columns using High-Strength Concrete," *Summaries of Technical Papers of Annual Meeting Architectural Institute of Japan*, C-2, 1997, pp. 25-26 (in Japanese).

[10] Ohno, Y., Miyamoato, Y.: "Effects of Details of End Hooks of Transverse Reinforcement on Structural Performance of Reinforced Concrete Columns," *Proceedings of the Japan Concrete Institute*, Vol. 20, No. 3, 1998, pp. 493-498 (in Japanese).

[11] Uwada, M., Nakazawa, A., Yamashita, Y., Miyakoshi, S., Kuwada, H., Minami, K.: "Experimental Study on Shear Behaviour of Reinforced Concrete Columns using High-Strength Shear Reinforcement of 8000 kgf/cm^2 Grade (Part 2)," *Summaries of Technical Papers of Annual Meeting Architectural Institute of Japan*, C-2, 1997, pp. 3-4 (in Japanese).

[12] Lynn, A.C., Moehle, J.P., Mahin, S.A., Holmes, W.T.: "Seismic Evaluation of Existing Reinforced Concrete Columns," *Earthquake Spectra*, V. 12, No. 4, Nov. 1996, pp. 715-739.

[13] Nakamura, T., Yoshimura, M.: "Gravity Load Collapse of Reinforced Concrete Columns with Brittle Failure Modes," *J. Asian Architecture and Building Engineering*, V. 1, No. 1, 2002, pp. 21-27.

[14] Sezen, H.: "Seismic Behavior and Modeling of Reinforced Concrete Building Columns," Ph.D. Thesis, University of California, Berkeley, 2000.

[15] Kabeyasawa, T., Tasai, A., Igarashi, S.: "An Economical and Efficient Method of Strengthening Reinforced Concrete Columns against Axial Load Collapse during Major Earthquake," *PEER Report*, 2002/2, pp. 399-411.

[16] Ousalem, H., Kabeyasawa, T., Tasai, A.: "Evaluation of Ultimate Deformation Capacity at Axial Load Collapse of Reinforced Concrete Columns," *13th World Conference on Earthquake Engineering*, Vancouver, British Columbia, Canada, 2004, Paper No. 370.

[17] Yoshimura, M., Takaine, Y., Nakamura, T.: "Collapse Drift of Reinforced Concrete Columns," *PEER Report*, 2003/11, *Fifth US-Japan Workshop on Performance-Based Earthquake Engineering Methodology for Reinforced Concrete Building Structures*, Hakone, Japan, 2003, pp. 239-253.

[18] Kogoma, I., Hayashida, T., Minowa, C.: "Experimental Studies on the Collapse of RC Columns During Strong Earthquake Motions," *10th World Conference on Earthquake Engineering*, Rotterdam, Holland, 1992, pp. 3013-3017.

[29] Itakura, Y., Yasui, K., Zhang, F., Masuo, K.: "Study on the Strength and Deformation Behaviors of R/C Beam Columns using High Strength Concrete," *Proceedings of the Japan Concrete Institute*, Vol. 14, No. 2, 1992, pp. 291-296 (in Japanese).

[20] Fukuhara, M., and Kokusho, S.: "Effectiveness of High Tension Shear Reinforcement in Reinforced Concrete Members," *Journal of Structural Construction Engineering*, AIJ, No. 320, 1982, pp. 12-20 (in Japanese).

[21] Arakawa, T.: "Allowable Shearing Stress and Shear Reinforcement for RC beams," *Summaries of Technical Papers of Annual Meeting Architectural Institute of Japan*, 1969, pp. 891-892 (in Japanese).

[22] ACI-318-11, *Building Code Requirements for Structural Concrete*, American Concrete Institute, Farmington Hills, Michigan, USA, 503 p.

[23] Bentz, E. C. and Collins, M. P.: *Response-2000*, Retrieved on May 5, 2015, from http://www.ecf.utoronto.ca/~bentz/r2k.htm

LIST OF TABLE AND FIGURE CAPTIONS

Table 1. Properties of Specimens (25.4mm=1in., 1MPa=145psi)

Ref No.	Unit	b (mm)	h (mm)	A_g/A_c	a/d	f'_c (MPa)	ρ (%)	f_y (MPa)	p_{we} (%)	f_{yt} (MPa)	$P/(bhf'_c)$	τ_n (MPa)	Controlling Limit**	τ_u (MPa)
6	P22N	250	250	1.35	2.07	29.3	4.95	1080	1.48	319	0	8.42	1	6.28
	P22S											8.42	1	6.69
7	1	250	250	1.29	2.22	19.9	1.63	360	0.10	740	0.20	2.57	2	1.95
8	2C	300	300	1.50	1.15	25.2	2.65	396	0.26	392	0.19	3.61	2	3.70
	3C										0.28	4.03	2	4.40
	2C13			1.54			1.69	350			0.19	3.54	2	4.45
9	1	250	250	1.35	1.13	98.7	3.82	999	0.60	757	0.13	11.7	2	11.9
	2										0.32	15.1	2	14.5
	3										0.51	17.2	1	15.9
	5								1.19		0.13	15.8	2	16.3
	6										0.32	20.5	2	17.7
	7										0.51	22.4	1	19.1
10	S-2	300	300	1.50	1.72	24.7	2.65	366	0.26	304	0.30	3.73	2	4.58
	S-4								0.52			4.80	2	4.67
11	B-1	300	300	1.19	1.63	20.7	3.54	685	0.22	832	0.30	4.15	2	3.85
	B-2				1.63				0.44			5.61	2	4.03
	B-4				1.09							5.61	2	4.44
12	3CLH18	457	457	1.52	3.74	26.9	3.04	331	0.08	400	0.09	2.28	2	1.97
	3CMD12*					27.6			0.21		0.26	3.93	2	2.58
	2SLH18					33.1	1.94		0.08		0.07	2.21	2	1.68
	3CMH18					27.6	3.04				0.26	3.03	2	2.46
	2CMH18					25.5	1.94				0.28	2.95	2	2.29
13	N18M	300	300	1.67	1.76	26.5	2.65	380	0.28	375	0.18	3.84	2	4.87
	N27C										0.27	4.32	2	4.87
	N27M											4.32	2	5.33
14	2CLD12M*	457	457	1.57	3.74	21.8	2.46	434	0.22	476	0.15	3.28	2	2.21
	2CLD12*					21.1					0.15	3.26	2	2.36
	2CHD12*										0.61	2.73	1	2.69
15	B-1	300	300	1.63	1.73	18.3	1.69	338	0.10	289	0.29	2.44	2	3.17
16	C1	300	300	1.63	1.73	13.5	1.69	340	0.10	587	0.30	2.52	2	2.90
	C4			1.61					0.36	384		3.29	1	3.06
	C8					18.0						3.97	2	4.17
	C12										0.20	3.47	2	3.89
	D1				1.15	27.7		447	0.54	398	0.22	5.33	2	6.11
	D16					26.1					0.23	5.28	2	6.12
	D11				1.73	28.2	2.26		0.18		0.21	3.62	2	4.35
	D12											3.62	2	4.48
	D13					26.1			0.54		0.23	5.34	2	4.76
	D14											5.34	2	5.30
17	1	300	300	1.67	2.35	30.7	2.65	402	0.28	392	0.20	4.33	2	4.33
	2								0.18			3.79	2	4.26
	3								0.14			3.49	2	4.26
	4								0.28		0.30	4.94	2	4.83
	5										0.35	5.18	1	5.09

Ref. No.	Unit	b (mm)	h (mm)	A_g/A_c	a/d	f'_c (MPa)	ρ (%)	f_y (MPa)	p_{we} (%)	f_{yt} (MPa)	$P/(bhf'_c)$	τ_n (MPa)	Controlling Limit**	τ_u (MPa)
[18]	CT1	130	130	1.82	4.05	22.8	4.71	355	0.23	355	0.18	3.65	2	2.69
[19]	C-3	317	317	1.46	1.21	57.7	2.02	433	0.36	878	0.47	9.86	1	9.77
	C-4			1.45					0.55	818		11.8	1	10.0
[20]	(2)-1&2	180	400	1.61	1.76	31.8	5.38	368	0	-	0	2.02	2	2.38
	(2)-3&4								0.38	250		3.53	2	4.47
	(2)-5&6									1322		6.95	2	6.93
	(2)-7&8								0.76	250		4.56	2	5.51
	(2)-9&10									1322		9.61	2	8.34
	(1)-1				1.18	27.6		343	0	-		1.95	2	2.25
	(1)-2								0.29	345		3.52	2	3.91
	(1)-3&4									1360		6.14	2	6.08
	(1)-6								0.40	345		3.98	2	4.61
	(1)-7									1360		7.17	2	7.56
	(1)-8								0.51	345		4.39	2	4.89
	(1)-9									1360		8.05	2	7.78
	(1)-10								0.74			9.19	1	9.03
	(1)-11								0.71	1413		9.20	1	8.36
	(1)-12								1.67			10.8	1	10.0

*contribution to transverse stress from inclined legs of hoops or ties computed using the components of the nominal forces in such legs in the direction of the applied lateral load.

** "Controlling Limit" shows whether Limit 1 or Limit 2 in Fig. 1 is used to determine shear strength.

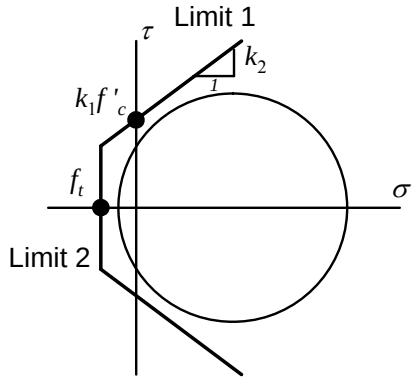

Figure 1. Failure Envelope

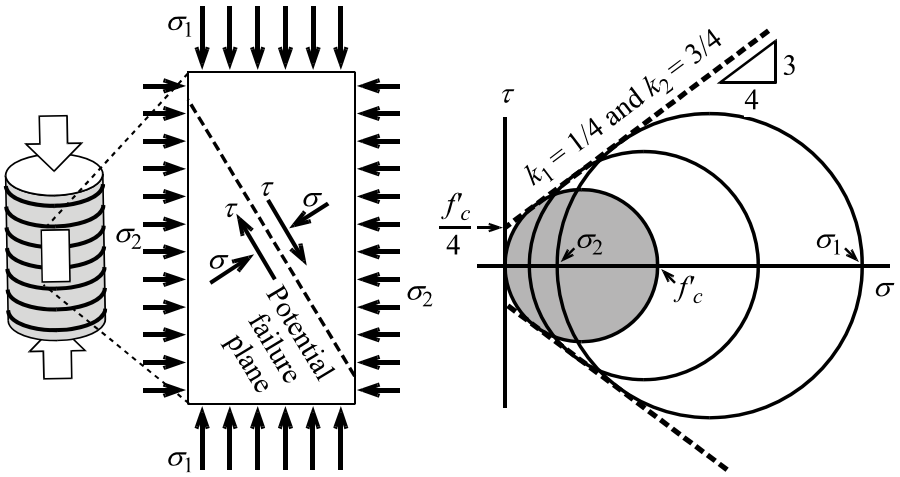

(a) Test of confined concrete (b) Tangent to circles described by Eq. 1

Figure 2. Failure criterion for confined concrete

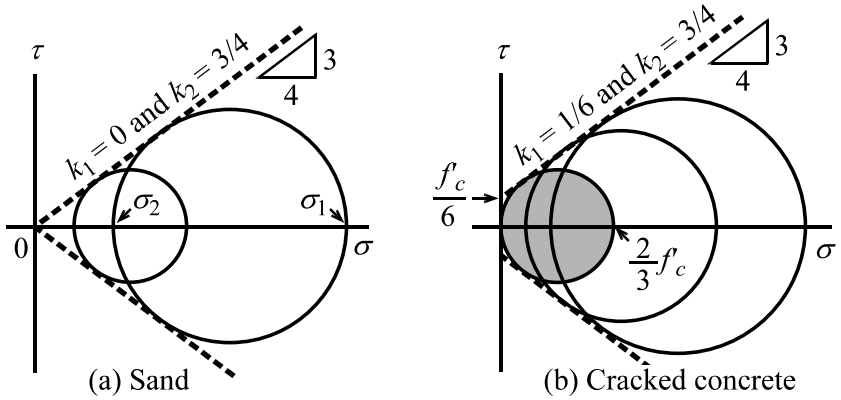

(a) Sand (b) Cracked concrete

Figure 3. Failure criteria for sand and cracked concrete

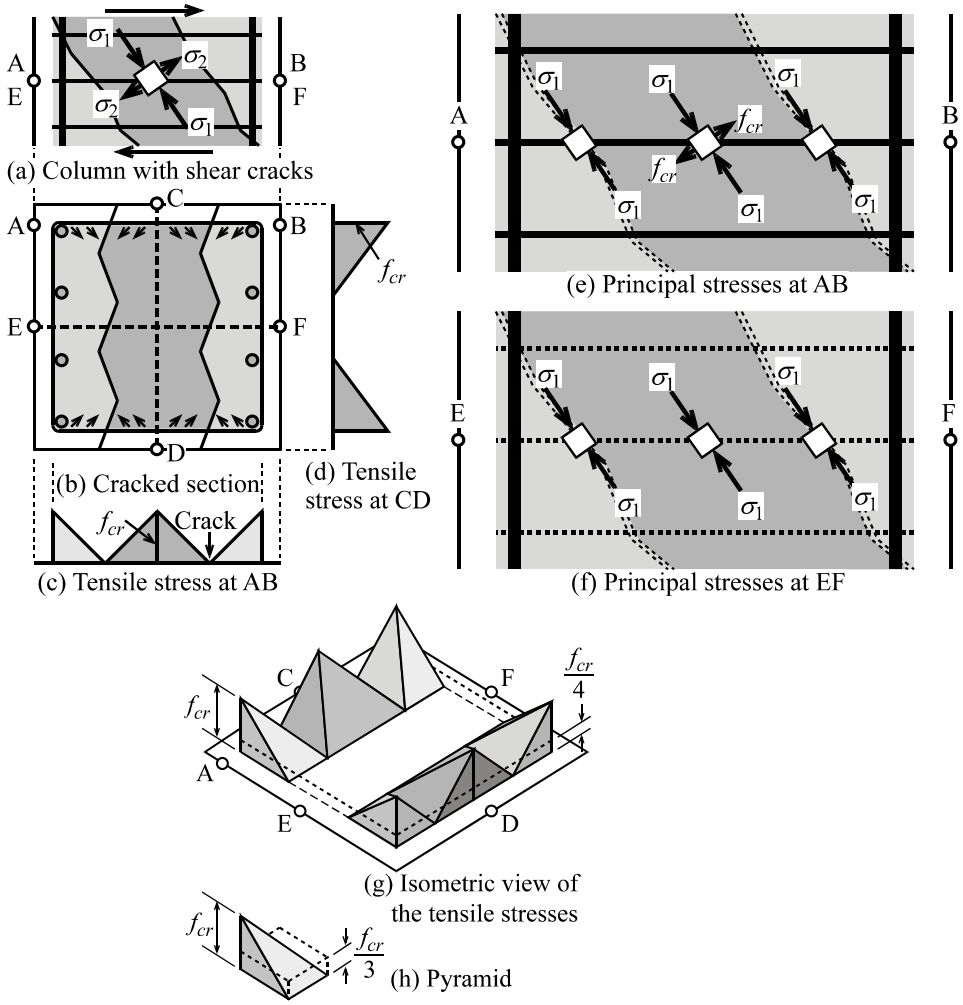

Figure 4. Idealized tensile stress in a column (Limit 2)

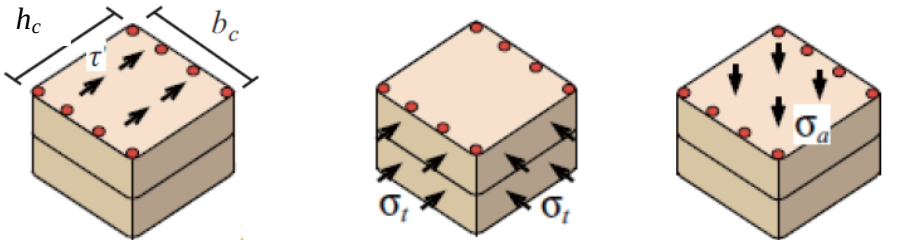

Figure 5. Definitions of mean stresses

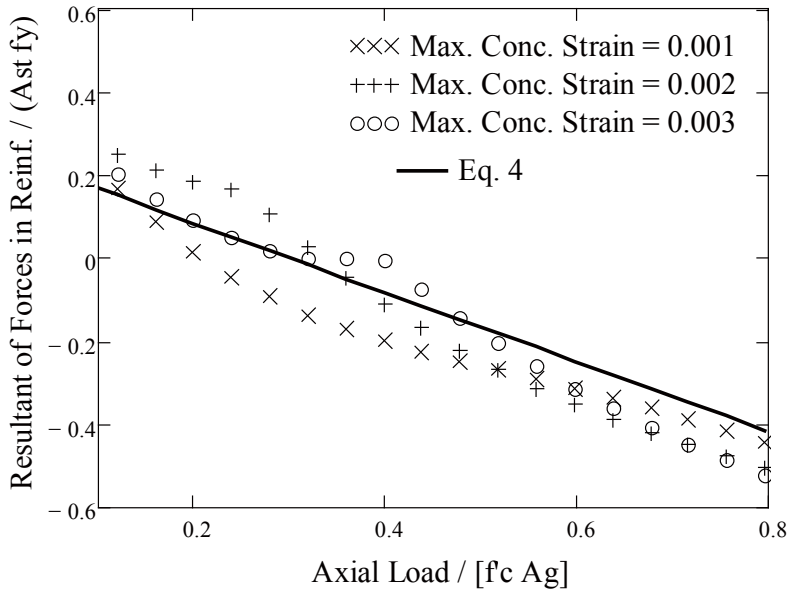

a) Section with two layers of reinforcement

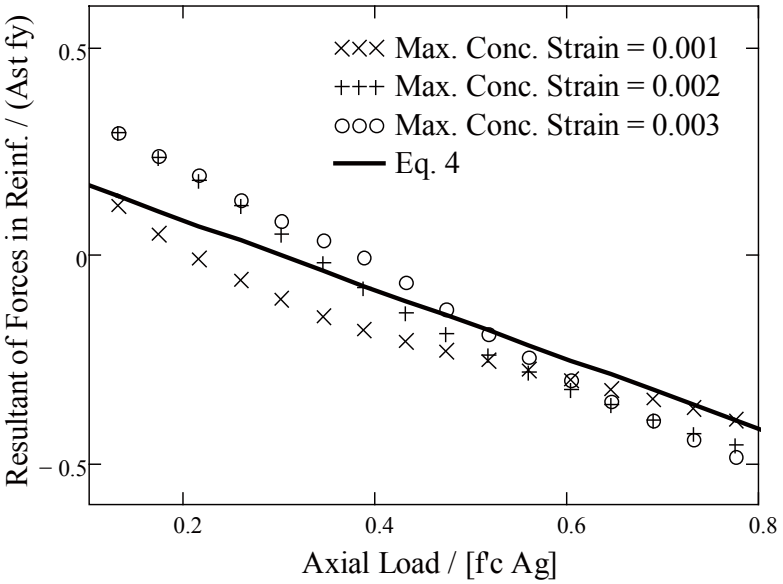

b) Section with four layers of reinforcement

Figure 6. Resultant forces in reinforcement of a section

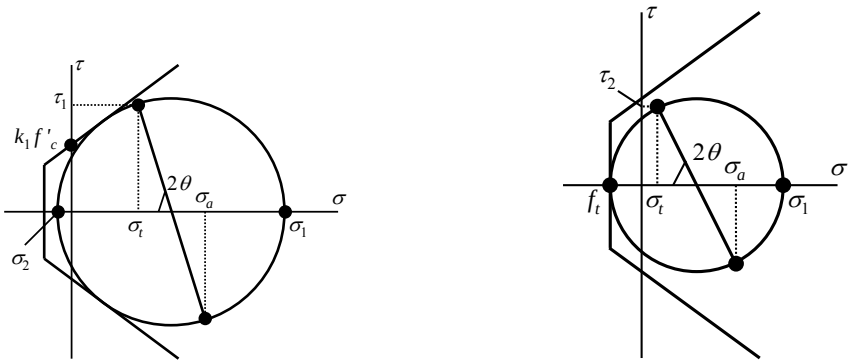

a) Case in which Limit 1 controls **b**) Case in which Limit 2 controls

Figure 7. Solutions

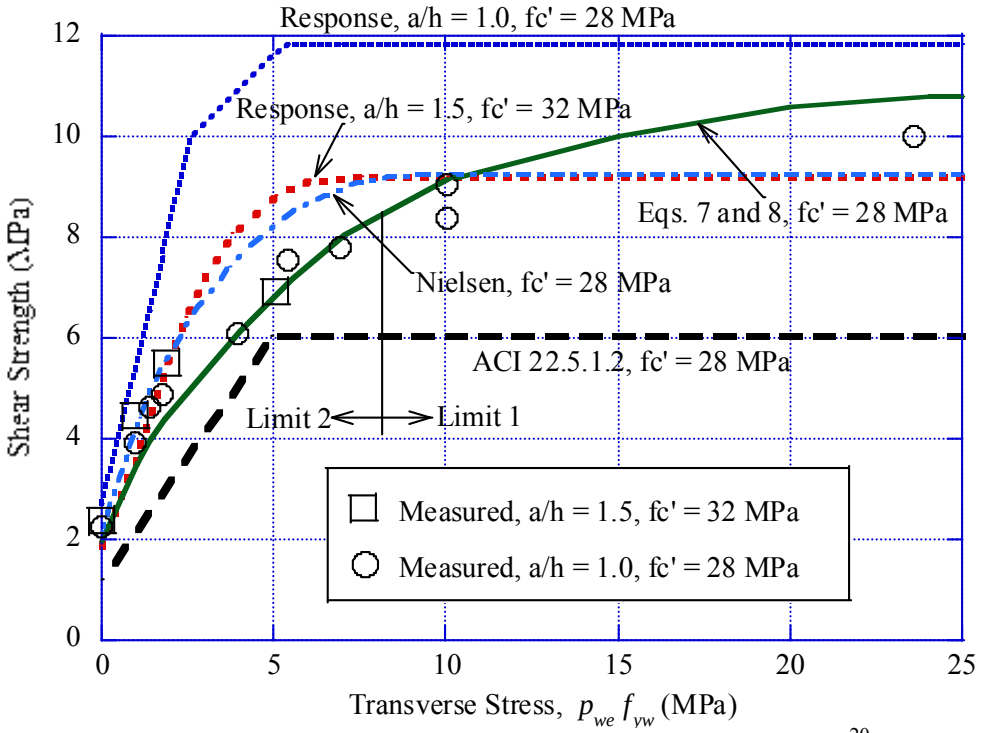

Figure 8. Comparisons with Results Reported by Fukuhara[20]

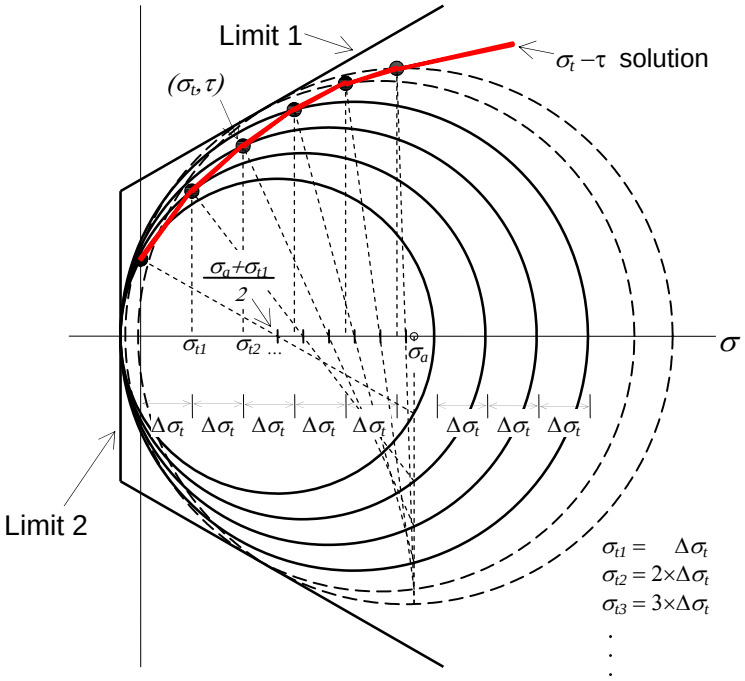

Figure 9. Mohr Circles for Increasing Transverse Stress and Constant Axial Stress

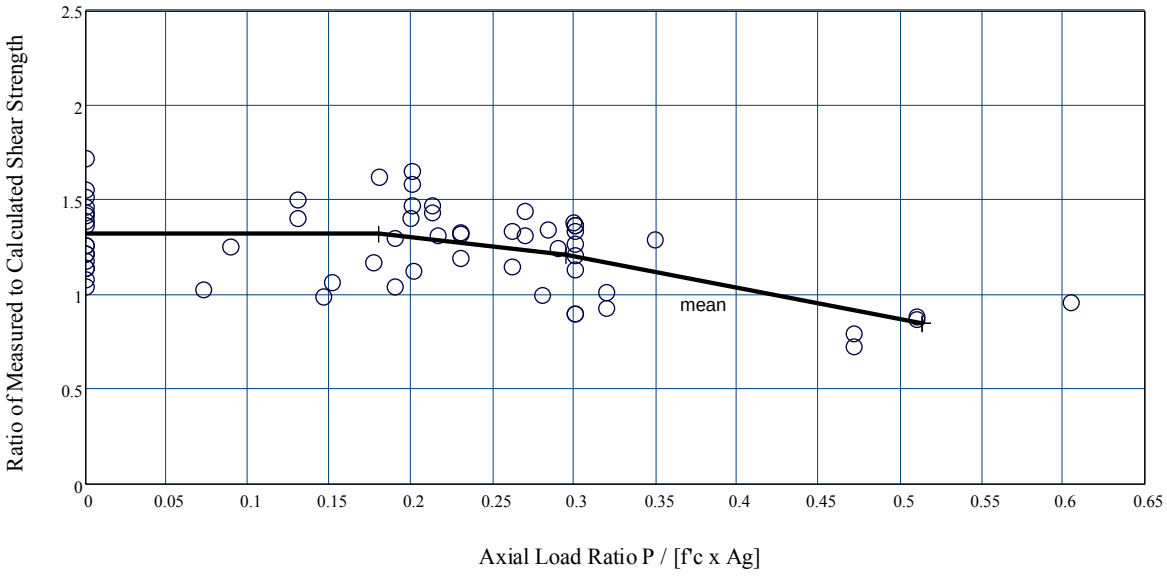

(a) Results from ACI Table 22.5.6.1(a)

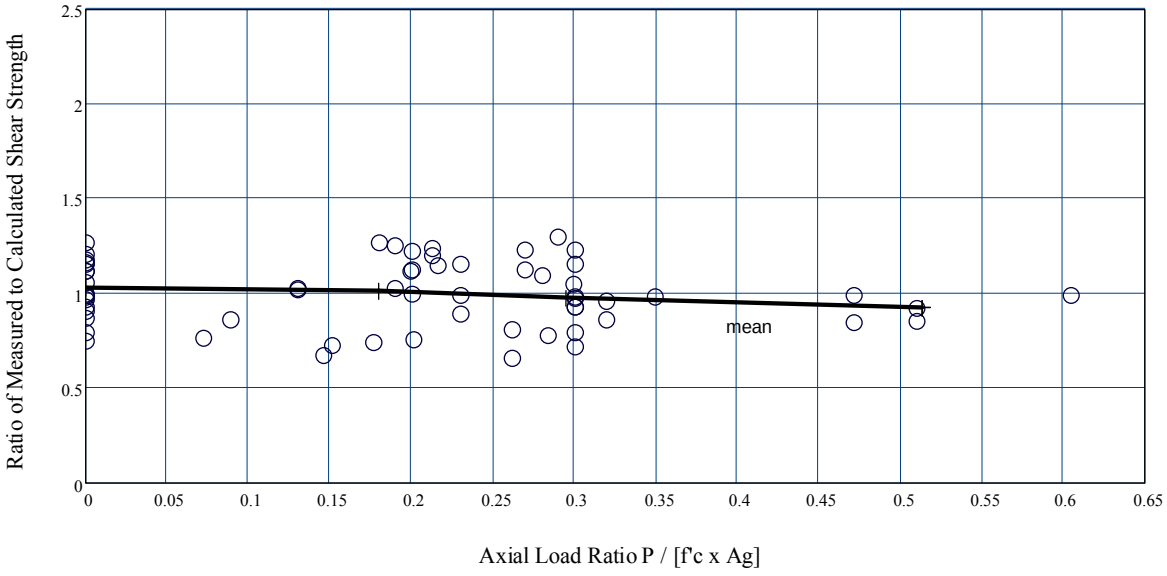

(b) Results from the proposed expression

Figure 10. Mean Ratios of Measured to Computed Shear Strength vs. Axial Load Ratio

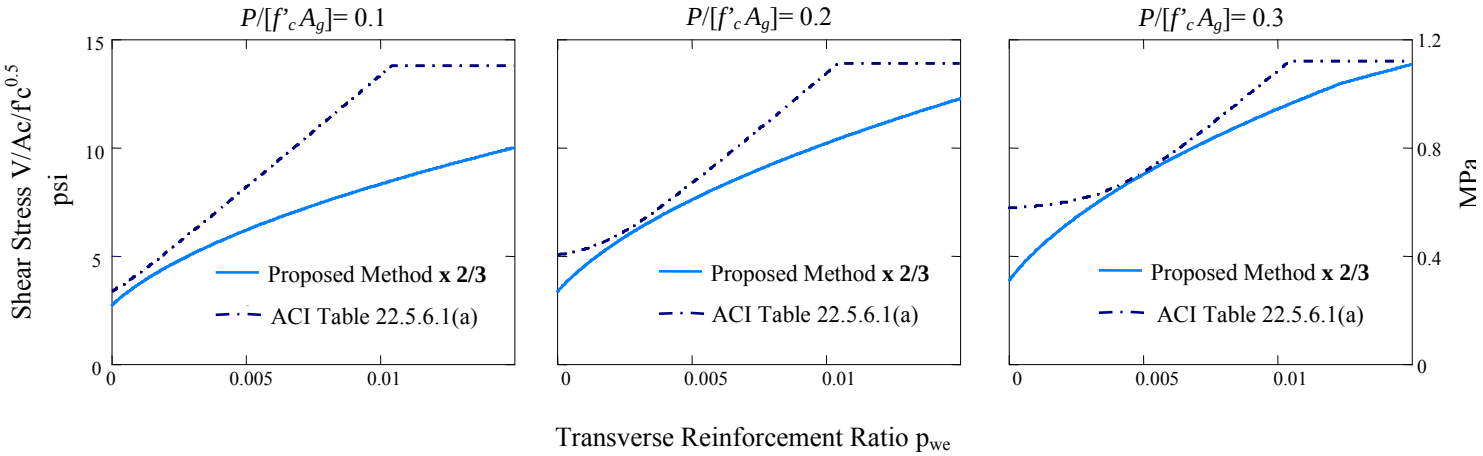

Figure 11. Comparisons of Projected Shear Strength

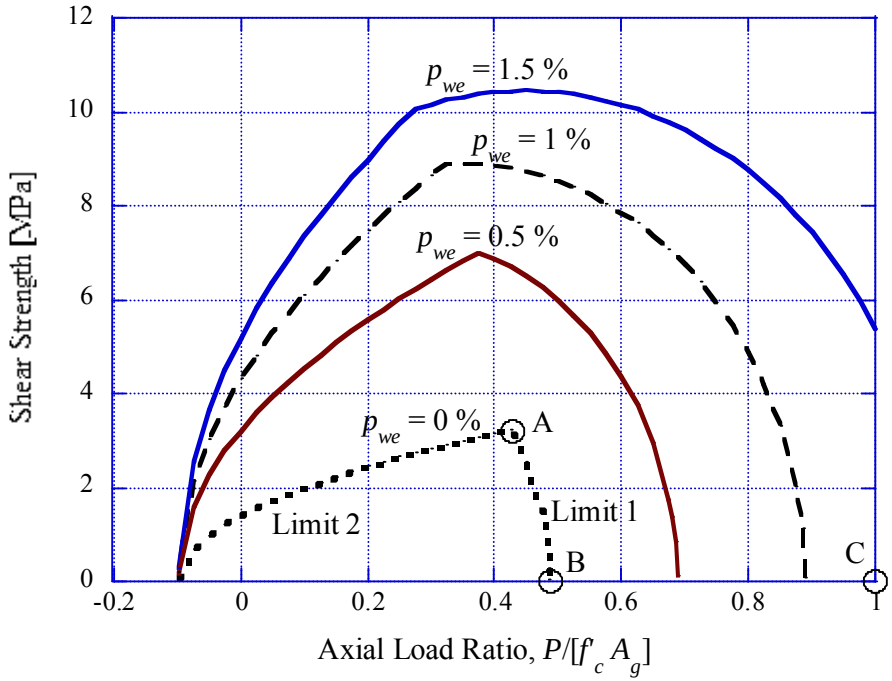

Figure 12. Relationship between axial load ratio and shear strength for various transverse reinforcement ratios

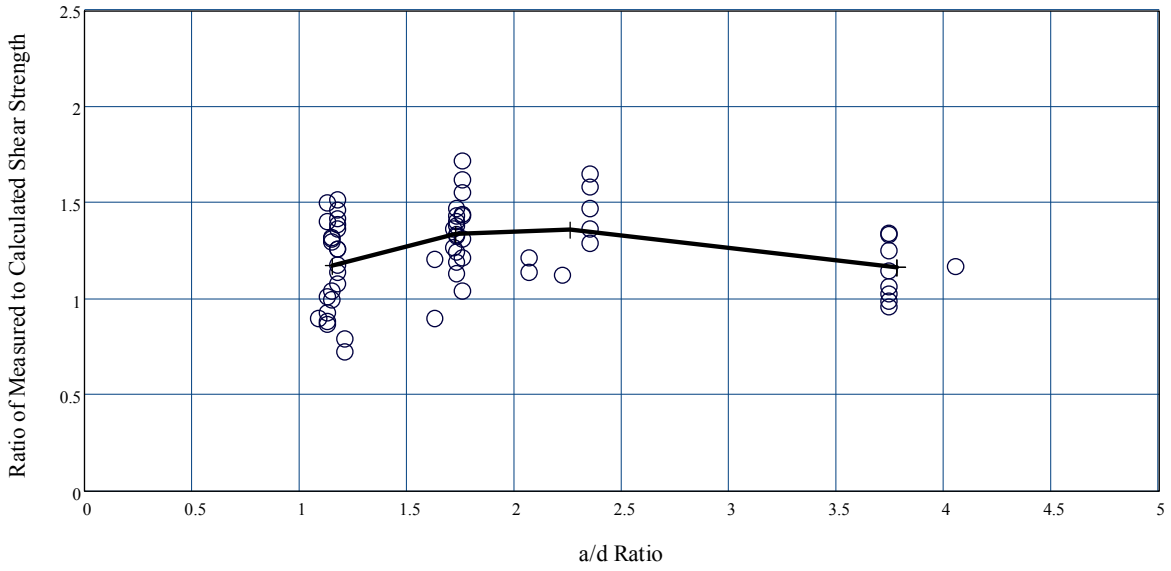

(a) Results from ACI Table 22.5.6.1(a)

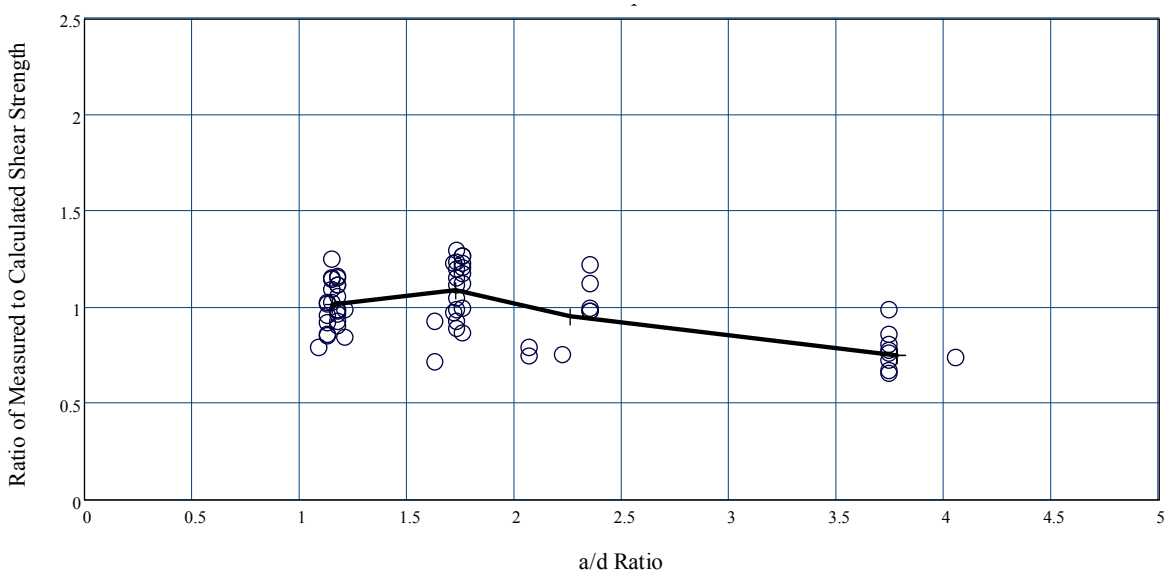

(b) Results from the proposed expression

Figure 13. Ratios of Measured to Computed Shear Strength vs. *a/d* Ratio